

JPRS: 27,511

TT: 64-51760

24 November 1964

*Metallovedenie i Termicheskaya Obrabotka*  
*Nr III 1964*

~~STRATEGIC METALS SCIENCE AND TECHNOLOGY~~

Edited by G. I. Pogodin-Alekseyev

- USSR -

*Inside Title*

SLAVIC LIBRARY  
BATTELLE MEMORIAL INSTITUTE  
COLUMBUS, OHIO

U. S. DEPARTMENT OF COMMERCE

OFFICE OF TECHNICAL SERVICES

JOINT PUBLICATIONS RESEARCH SERVICE

Building Tempo E

East Adams Drive, 4th & 6th Streets, S.W.

Washington, D. C. 20443

Price: \$4.00

REPRODUCED FROM  
BEST AVAILABLE COPY

**DISTRIBUTION STATEMENT A**  
Approved for Public Release  
Distribution Unlimited

20010906 065

61138

# MECHANISM FOR THE FORMATION AND PROPERTIES OF A BORATED LAYER IN IRON AND NICKEL ALLOY

Doctor of Technical Sciences Prof Yu.M. Lakhtin  
and Engineer M.A. Pchelkina

Pages 42-63

## The Boration of Iron and its Alloys

Iron with boron forms solid solution and the two borides  $\text{Fe}_2\text{B}$  and  $\text{FeB}$ . Fig 1 shows a diagram for the composition Fe-B, constructed from data given by several authors (Ref 1-4) and (12-17).

The solubility of boron in  $\alpha$ - and  $\gamma$ - iron according to Vesper and Muller (Ref 12) depending on the temperature is given in Table 1.

Table 1.

(a) Модифика- ция железа	(b) Температура в °C			
	1381	1174	915	880
$\alpha$	0,15	—	0,15	0,1
$\gamma$	0,1	0,15	0,1	—

a) modification of iron; b) temperature in degrees C.

More recent studies of the FeB system have confirmed the presence in it of boride phases of the type  $\text{Fe}_2\text{B}$  and  $\text{FeB}$ ; there are significant differences in the data on the solubility of boron in  $\alpha$ - and  $\gamma$ -iron. Thus, Spretnik and Speizer (Ref 13) have indicated that the solubility of boron in iron at a temperature of 970°C does not exceed 0.003%.

Nikolson (Ref 14) feels that the maximum solubility of boron in  $\gamma$ -iron is at a temperature of 1,165°C 0.0021%, decreasing to 0.001% at 911°C. At a temperature of 911°C the solubility of boron in  $\alpha$ -iron is 0.002%, decreasing with a decrease in temperature.

A higher solubility of boron in iron was obtained in the studies of Basbi and others (Ref 15), (Ref 16). In  $\gamma$ -iron it amounts to 0.0035% at a temperature of 982°C and in  $\alpha$ -iron it changed within the following range as a function of temperature:

Temperature in degrees C	850	835	751	700
Solubility in percent	0.0035	0.0018	0.0006	0.0003

McBrady, Spretnik, and Speizer (Ref 17) carried out careful studies of the Fe-B system. They smelted the metals to be studied in an induction furnace in a vacuum or in a furnace with controlled atmosphere electrolytic iron and boron having a high degree of purity, obtained as a result of  $\text{BCl}_3$  dissociation, were used as the initial materials. As a result of the study, a part of the FeB composition diagram was constructed, shown in Figure 2, which apparently is the closest to reality.

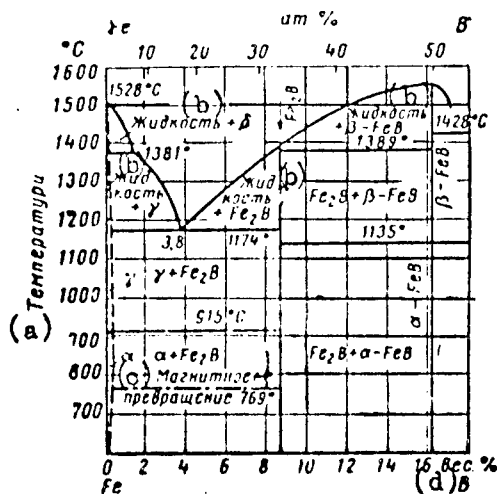


Fig 1., FeB composition diagram.  
a) temperature; b) liquid;  
o) magnetic conversion; d) weight %.

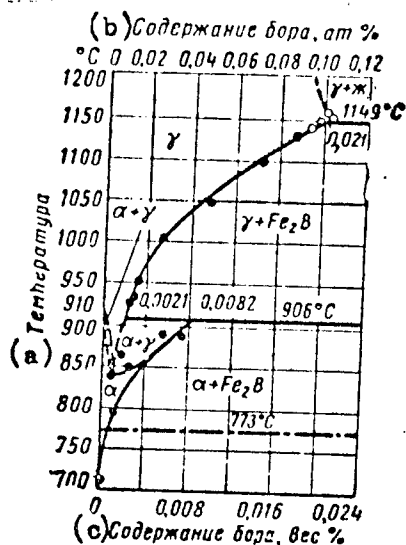


Fig 2. Fe-B composition diagram.  
a) temperature; b) boron content  
in percent; c) boron content in  
weight percent.

Table 2

(a) Модификация железа	(b) Температура в °C										
	1131	1103	1049	1008	951	919	906	887	835	794	710
γ	0,0182	0,0143	0,0089	0,0061	0,0034	0,0021	—	—	—	—	—
α	—	—	—	—	—	—	0,0082	0,0061	0,001	0,0011	0,0002

a) modification of iron; b) temperature  
in degrees C.

Several authors (Ref 17) and (Ref 18) have felt that with  $\alpha$ -iron boron forms a solid solution of introduction, and with  $\gamma$ -iron - of substitution. Measurement of base vapor pressure however showed that during dissolution of boron in  $\gamma$ -iron the formation of a solid solution of introduction was possible. This question requires further study. It is most probable that boron is preferably located at defects in the lattice, particularly at the boundaries of the grains.

All those studying the Fe-B system have not noted regions of solid solutions at the base of iron borides (see Fig 1), taking into account their pure chemical compounds

which are not soluble in boron or in iron.

[Starting with the Fe-B system and a general theory for the formation of a multiphase diffusion layer, in the saturation of iron or another metal by a diffusing element it is possible to represent the formation kinetics of the borated layer in iron in the following way, (Ref 2).

[Depending on the temperature, the saturation of boron first diffuses in  $\alpha$ - or  $\gamma$ - iron up to complete saturation. After the maximum solubility of boron in  $\alpha(\gamma)$  - iron is reached seeds of the boride  $\text{Fe}_2\text{B}$ , which is stable at a different temperature, are formed on the surface of the iron. This boride takes the form of specific needle-like crystals going from the surface to the interior. As time passes seeds of the boride  $\text{FeB}$  are formed on the surface of the iron, which take the form of needle-like crystals.] A typical structure of a borated layer, obtained in iron is shown in Figure 3. [This type of a diffused layer is probably connected with the varying, non-uniform formation of seeds of the boride phases on the surface and with the great rapidity of their diffusion growth as compared to the lateral growth. During the transition from one phase to another a sharp drop in the boron concentration (Ref 5) can be observed in the diffusion layer. The formation of boride layers during the saturation of iron by boron cannot be explained, assuming the possibility of instability in the composition of the boride phases.]

Fig. 4



Fig 3. Microstructure of a borated layer in technical iron. X300

There is no doubt that borides are solid solutions. Consequently, it is impossible to draw vertical lines (Fig 1) which correspond to the chemical composition of  $\text{Fe}_2\text{B}$  or  $\text{FeB}$  in a diagram for the Fe-B composition, and it is necessary to designate the areas in which these phases exist. The homogeneity limits of boride phases must be the subject of a special study.

Figure 4 indicates the dependence of the over-all depth of the diffusion layer and of the zone of solid borides on the saturation temperature. As can be seen from Figure 4 a break in the curve can be observed in the transition from  $\alpha$ - to  $\gamma$ - phase. Apparently, this can be explained by the fact that in the  $\alpha$ - phase the diffusion process is carried out much more easily than in the  $\gamma$ - phase (Ref 5).

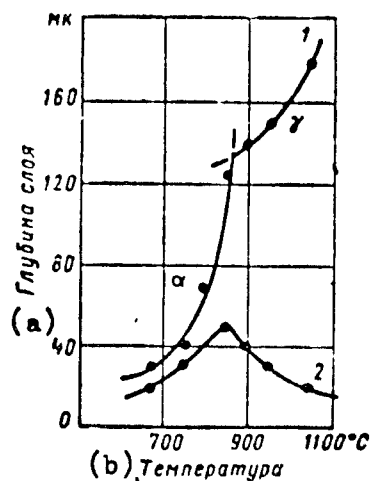


Fig 4. Effect of temperature on the depth of the borated layer in technical iron. Diborane medium with hydrogen for 2 hours: 1 - general layer depth; 2 - depth of the solid layer of borides. -- a) Layer depth; b) Temperature.

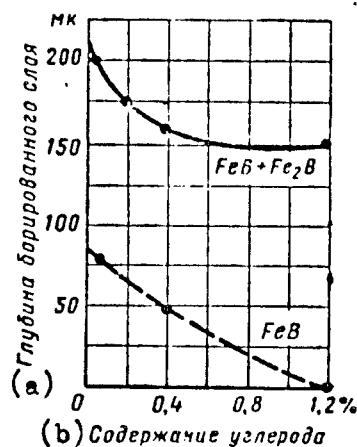


Fig 5. Effect of the carbon content in steel, subjected to boration upon the depth of the borated layer. a) depth of the borated layers; b) carbon content.

Carbon retards the diffusion of boron in iron which can be readily seen in Figure 5, while an increase of carbon in steel decreases the development of the boride FeB. The hardness of the borated layer decreases with an increase of carbon in the original steel (Table 3).

Table 3

(a) Содержа- ние в стали углерода в %	(b) Твердость боридов	
	FeB	Fe <sub>2</sub> B
0,06	2290	2000
0,22	2250	1780
0,40	2010	1530
1,2	1890	—

- a) carbon content in the steel in percent;  
b) hardness of the borides.

According to several studies (Ref 6-8), boron with carbon forms a carbide of the type  $B_{12}C_3$  ( $B_4C$ ). However, along with the studies of other authors (Ref 4), our studies (Ref 5) have shown that when steel is saturated with boron boron carbides are not formed in the diffusion layer on the other hand, in the formation of boride phases the displacement of carbon from the surface in the direction of the diffusion is often observed, which leads to the formation of a zone with a higher carbon content ahead of the front of growing borides (Figure 6). Thus, a perlite structure is observed behind the layer of borides on the surface of steel containing an average amount of carbon. This structure gradually changes into the original perlite-ferrite structure of hypoeutectoid steel. A grain of austenite, which is enriched by boron (which is in solid solution) and by carbon, is much larger than in the sample core (see Figure 6).

There is a great deal of interest in the boration of alloyed steel, including highly alloyed steel which belongs to the ferrite and austenite class. The introduction of alloy components into steel, particularly elements of a transition group, had a great effect upon the phase composition of the diffusion layer, on the kinetics of its formation, and in technical characteristics of the layer - the depth, the hardness, the resistance to erosion, and corrosion.

In Table 4 an attempt is made to systematize the borides phases which are formed from the interaction of boron with different elements from the periodic element system of Mendeleev according to data in the literature.  
[Note: Table 4 is not reproduced for this report.]





Fig 6. Microstructure of the borated steel layer 45 (boration temperature 750°C. X200).

In the formation of compounds of B with transitional refractory metals from the IV, V, and VI group of the periodic system of elements, the degree to which the unfinished d-levels of the atoms are filled by electrons from boron atoms is greater, the lower are the energy characteristics and the greater is the electronic defect of the d-level of the transition metal (Ref 9).

In the change from one metal in a group of the periodic system to another, the probability that p-electrons of boron will remain at the location of unfilled d-electronic sublevels of transition metal atoms increases approximately proportionally to the number of electrons which are found in the d-electronic sublevel and to the main quantum number of this level, i.e., proportionally to  $1/Nn$  (Ref 17).

The reason that certain metals do not form borides can be found in their electronic structure, since it is not possible to explain this phenomenon by differences in the radii and ionization potential of the metals. In the boride  $Me_4B$  and  $Me_2B$ , the electronic interaction of isolated B atoms with metal atoms which form the lattice are very weak and consist of the transmission of electrons from the metal to boron with subsequent overlapping of the filled p and  $Sp^3$  - hybrid (for  $Me_2B$ ) orbits of B and of the empty p- or d -

orbits of the closest metal atoms. This type of interaction is characteristic for transitional metals.  $Sp^3$  - hybridization takes place for  $MeB$  borides, where in a zigzaglike chain of B atoms each atom forms two bonds B - B and two bonds B - Me. In  $MeB_2$  borides the B atoms form hexagonal flat lattices and are connected with each other by  $Sp^2$  - orbits; these are connected with metallic lattice by means of the p - orbit. The  $MeB_6$  and  $MeB_{12}$  borides are composed of metal atoms and aggregates of  $B_6$  and  $MeB_{12}$ ; electronic interaction leads to the transmission of metal electrons in these aggregates. The question as to the existence of this type of borides is determined by the value for the potential and the radius of the metal.

In order to clarify the effect of component alloys on the phase composition, the formation mechanism, the depth and the properties of the borated layer, we carried out a special study. Steel containing an average amount of carbon (0.38 - 0.51% C) with varying chromium content (from 1.06 to 25.5%) and nickel content (from 2 to 12.8%) was subjected to boration. In addition, we studied the effect of the nickel content (2-8%), the manganese content (1.96-8%) upon the boration of steel containing a large amount of chromium, with chromium content of 15% and 45%, and also the effect of tungsten, titanium (1.9-3.5%) and niobium (0.6-1.54%) in the boration of steel of the Kh18N8 type.

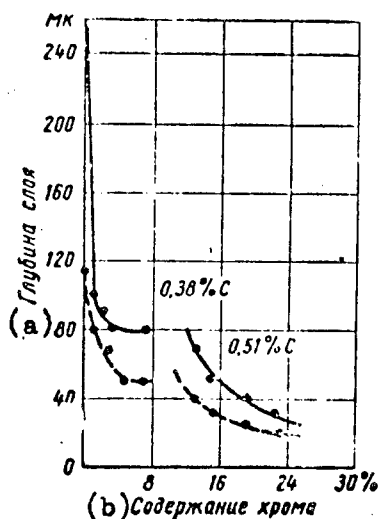


Fig 7. The effect of chromium on the depth of the borated layer. a) depth of layer; b) chromium content.

With the exception of steel containing a large amount of chromium, all of the steel had a austenitic structure at a given boration temperature, at the saturation temperature steel containing a large amount of chromium had a mixed structure consisting of  $\alpha$ - plus  $\gamma$ - phases.

Data on the effect of chromium on the depth of the borated layer are given in Figure 7. The distance from the sample surface to the end of the boride phases, including the transitional layer (solid solution plus borides) - if it was observed in the structure - was taken as the full layer depth.

At the same time the depth of the solid layer of borides was measured. The data obtained showed that the addition of chromium up to 3% in the steel containing an average amount of carbon greatly decreased the depth of the diffusion layer (see Fig 7).

A further increase in chromium from 3-8% did not cause any noticable change either in the over-all layer depth or of the layer of solid borides.

With a high chromium content (12-25%) in steel having a content of 0.51%C, a further decrease in the depth of the borated layer was observed (see Fig 7).

Under the effect of chromium the microhardness of the borated layer increased somewhat. Thus for example the microhardness of steel containing 0.38%C and 0.06%Cr was H<sub>200</sub> 1290, while for an increase of chromium up to 7.56% - H<sub>200</sub> 1850. In steel containing 0.51%C and 13.0-19.5%Cr, the microhardness fell within the range H<sub>200</sub> 1850-2290.

Up to 4-6% nickel (Fig 8) lowers the depth of diffusion layer. With a higher nickel content, the over-all depth of the layer barely changes, but the depth of the solid boride layer sharply decreases. This can be readily seen in Figure 9, where the microstructures of a borated layer in nickel steels are shown. Some times the penetration of boride "moustaches" (Fig 9) was observed in nickel steel at a considerably large depth as compared with the measured depth of the borated layer (Fig 8).

In steel having a large nickel content (6-8%) there is practically no solid boride layer and only a austenitic - boride zone is observed (Fig 9). If the amount of nickel in the steel is increased the hardness of the borated layer decreases.

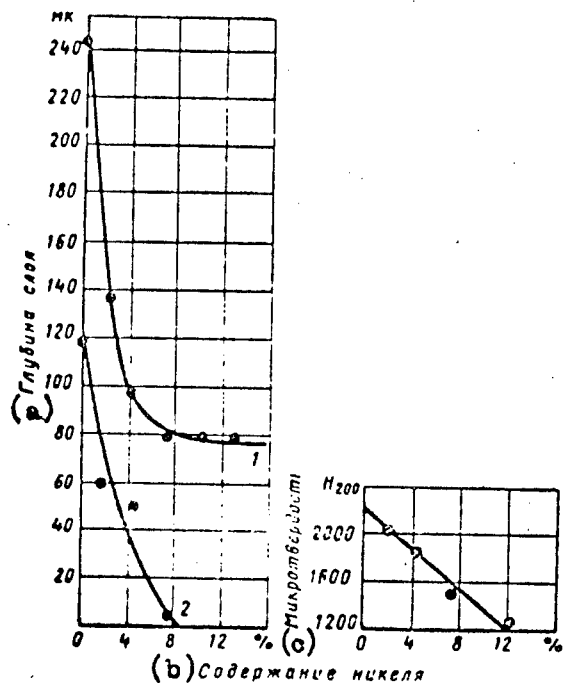


Fig 8. Effect of nickel on the depth of the borated steel layer containing 0.41%C. a) layer depth; b) nickel content; c) microhardness.

If steel containing a large amount of chromium is alloyed with nickel (0.32%C, 15.52%Cr), a certain increase in the over-all depth and the depth of the solid borides is observed. With a higher nickel content the layer depth either does not change or decreases only slightly (Fig 10). The structure of the diffusion layer can be seen in Figure 11. A well developed layer of solid borides can be observed in all the steel. The presence of tungsten (2.2%) in steel containing a large amount of chromium lowers the depth of the borated layer.

The introduction into chromium steel (0.32%C and 15%Cr) of up to 8% manganese barely changes the depth or the structure of the borated layer.



Fig. 9. Microstructure of a borated layer of steel, containing C = 0.41%; Ni = 12.82%. X300

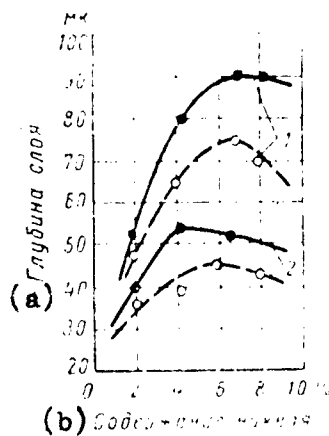


Fig. 10. Effect of nickel on the depth of the borated layer of steel, containing: 1 -- 0.32% C, 15.52% Cr; 2 -- 0.32% C, 15.52% Cr and 2.2% W.  
a) Layer depth; b) Nickel content.

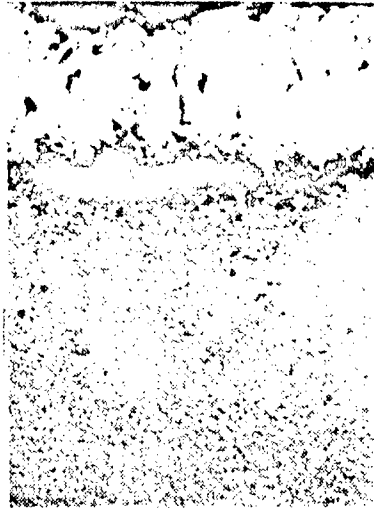


Fig 11. Microstructure of the borated layer in steel containing 0.32%C, 15.52%Cr and 8.0%Ni. X300

Figures 12 and 13 show the effect of titanium and niobium on the depth and microhardness of the borated layer in steel of the Kh18N8 type. It can be seen from the data which I presented that niobium and especially titanium, greatly decrease the depth of the borated layer and decrease its hardness. The decrease in the depth of the diffusion layer under the effect of alloy components is apparently connected with the increase in the stability of the bond in the boride, which was shown experimentally in the boration of alloyed ferrite (Ref 14).

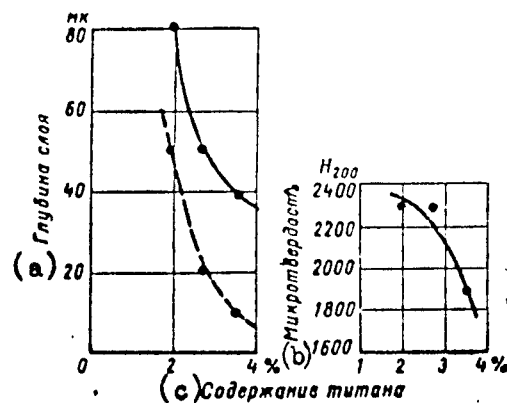


Fig 12. The effect of titanium on the depth and hardness of the borated layer in Kh18N8 steel. a) layer depth; b) microhardness; c) Titanium content.

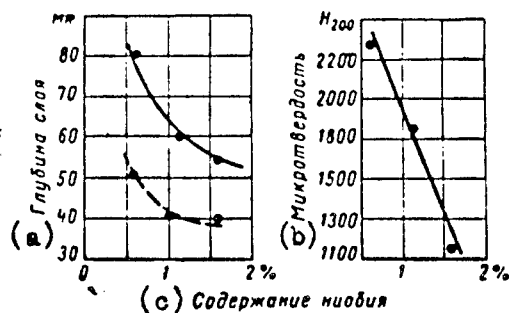


Fig 13. The effect of niobium on the depth and hardness of the borated layer of Kh18N8 steel. a) layer depth; b) microhardness; c) Niobium content.

Along with studying the effect of different elements on the boration process, we made a study of the boration of a series of standard heat resistant, fire resistant and rust resistant brands of steel. The data shown in Table 5 show that practically all of the steel studied could be strengthened by the boration method.

Table 5

(a) Марка стали	(b) Режим борирования		(c) Глубина слоя в мк		(h) Микро- твердость H <sub>100</sub>
	(d) Температура в °C	(e) Продолжи- те льность в ч	(f) сплошных боридов	(g) общий	
15X11MФ (i)	850	6	100—120	140	2290
25X2MФ (j)	850	6	40	40	1144
15X11MФ (i)	850	6	24	24	1006— 1072
X25T (k)	850	6	—	—	—
X18H9T (l)	950	6	25	100	2200
X18H25C2 (m)	900	4	25	115	1300
X23H18 (n)	950	6	15	130	1510
X25H20C (o)	950	6	15	70	1510
X25H25T (p)	950	6	12	130	1290
X15H37B3T (q)	850	6	30	80	2190

a) brand of steel; b) boration regime; c) layer depth in mk;  
d) temperature in degrees C; e) duration in hours; f) solid  
borides; g) total; h) microhardness; i) 15Kh11MF; j) 25Kh2MF;  
k) Kh25T; l) Kh18N9T; m) Kh18N25S2; n) Kh23N18; o) Kh25N20S;  
p) Kh25N25T; q) Kh15N37V3T.

In Figures 14 - 16 we have shown the effect of temperature on the duration of boration on the depth of the diffusion layer of perlitic steel 20KhNMF, of steel belonging to the martensite-ferrite class 15Kh11MF, 25Kh2MF, of ferrite steel Kh25T and austenitic Kh15N37V3T. As would be expected, with an increase in temperature and duration of the process, the layer depth increased. The possibility was thus revealed of borating the steel being studied at comparatively low temperatures (700-850°C), which is of great practical interest not only from the point of view of simplifying technology but also from the point of view of preserving the essential



properties. Thus for example steel 15Kh11MF is subjected to tempering at 750°C, and consequently boration, which is the final operation in preparing it, must be carried out at a temperature not exceeding 750°C.

Studies carried out by A. V. Ratner and L. G. Leonova at the Institute Imeni F. E. Dzerzhinskiy showed that boration of a layer obtained after saturation in a  $B_2H_6$  plus  $H_2$  medium in Kh15N3V3T steel had a high resistance to erosion and to scratching, after being heated for a long period of time (1750 hours) at a temperature of 700°C.

Figure 17 shows the distribution of microhardness according to the depth of the borated steel layer Kh15N37V3T. Within the limits of the solid layer of borides the hardness barely changes; with the transition into the austenitic - boride zone, the microhardness sharply decreases. The nature of the hardness distribution depending on the depth of the borated layer in other brands of steel which have been studied is completely similar to that shown in Figure 17. Long heating of the austenitic steel of the type Kh15N37V3T at a temperature of 700°C barely changes the microhardness of the diffusion layer.

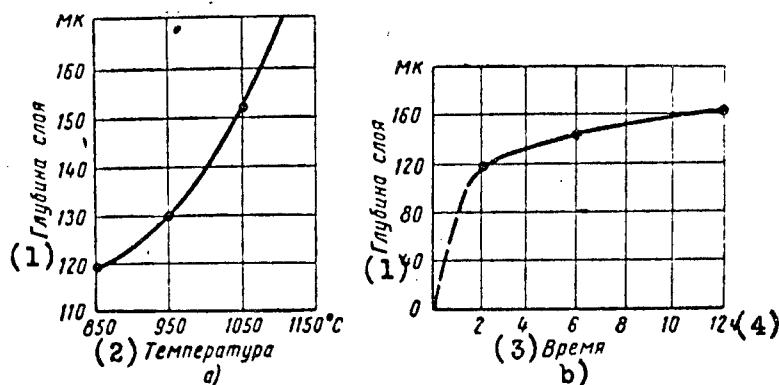


Fig 14. Effect of temperature (a) and duration of the process (b) on the depth of the borated layer of 20KhNMF steel.  
1) layer depth; 2) temperature; 3) Time;  
4) hours.

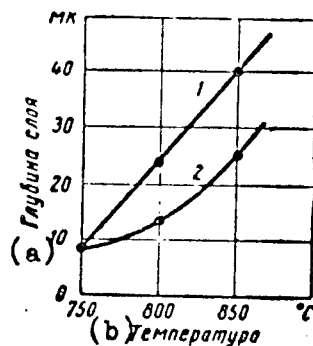


Fig 15. Effect of temperature on the depth of the borated layer: 1 - 15Kh11MF steel; 2 - 25Kh2MF steel.  
a) layer depth; b) temperature.

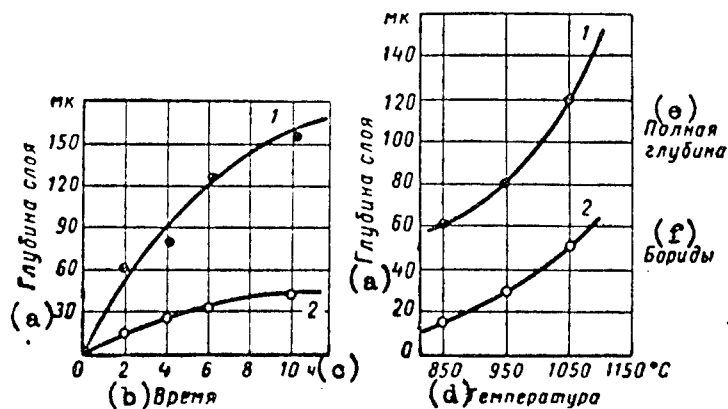


Fig. 16. Effect of temperature (A) and duration of boration at 850°C (B) on the layer depth of Kh15N37V3T steel: 1 -- total layer depth; 2 -- zone of solid borides.  
a) layer depth; b) time; c) hours; d) temperature; e) total depth; f) borides.

The formation kinetics of the borated layer in alloyed steel differs from the formation kinetics of a layer in iron or another pure metal. At the temperature at which

iron or another metal is saturated by boron phase mixtures cannot occur, for example  $\gamma(\alpha)$  - solid solution of borides. If there are component alloys in the original steel, especially boride producing components, then a multiphased layer can be formed at the diffusion temperature - a saturated  $\alpha(\gamma)$  - solution and borides.

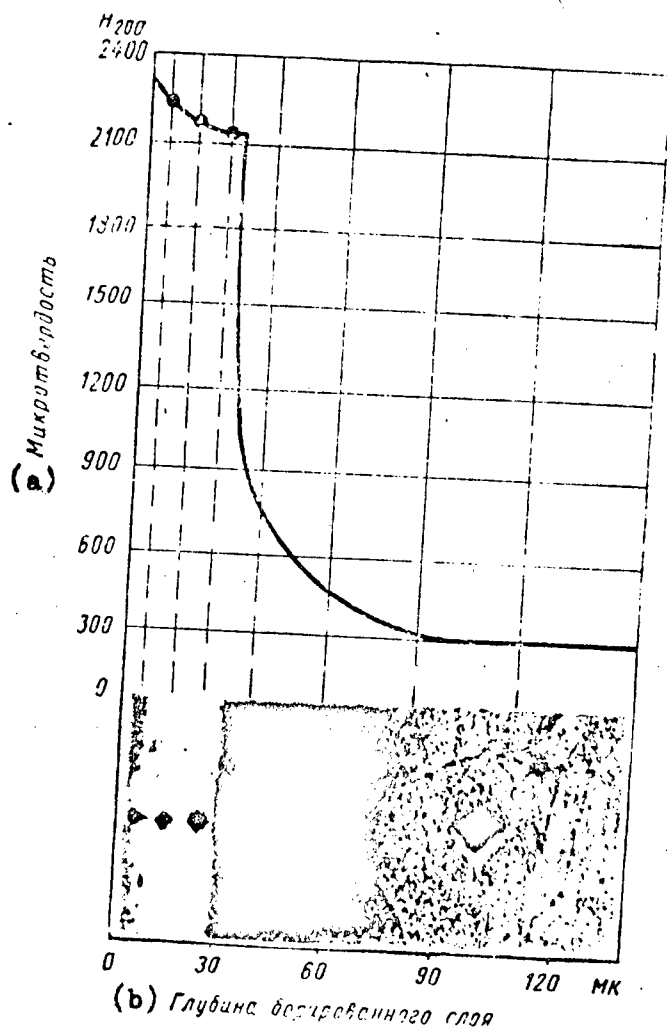


Fig 17. Hardness distribution according to borated layer of steel Kh15N37V3T; X500. a) microhardness; b) depth of borated layer.

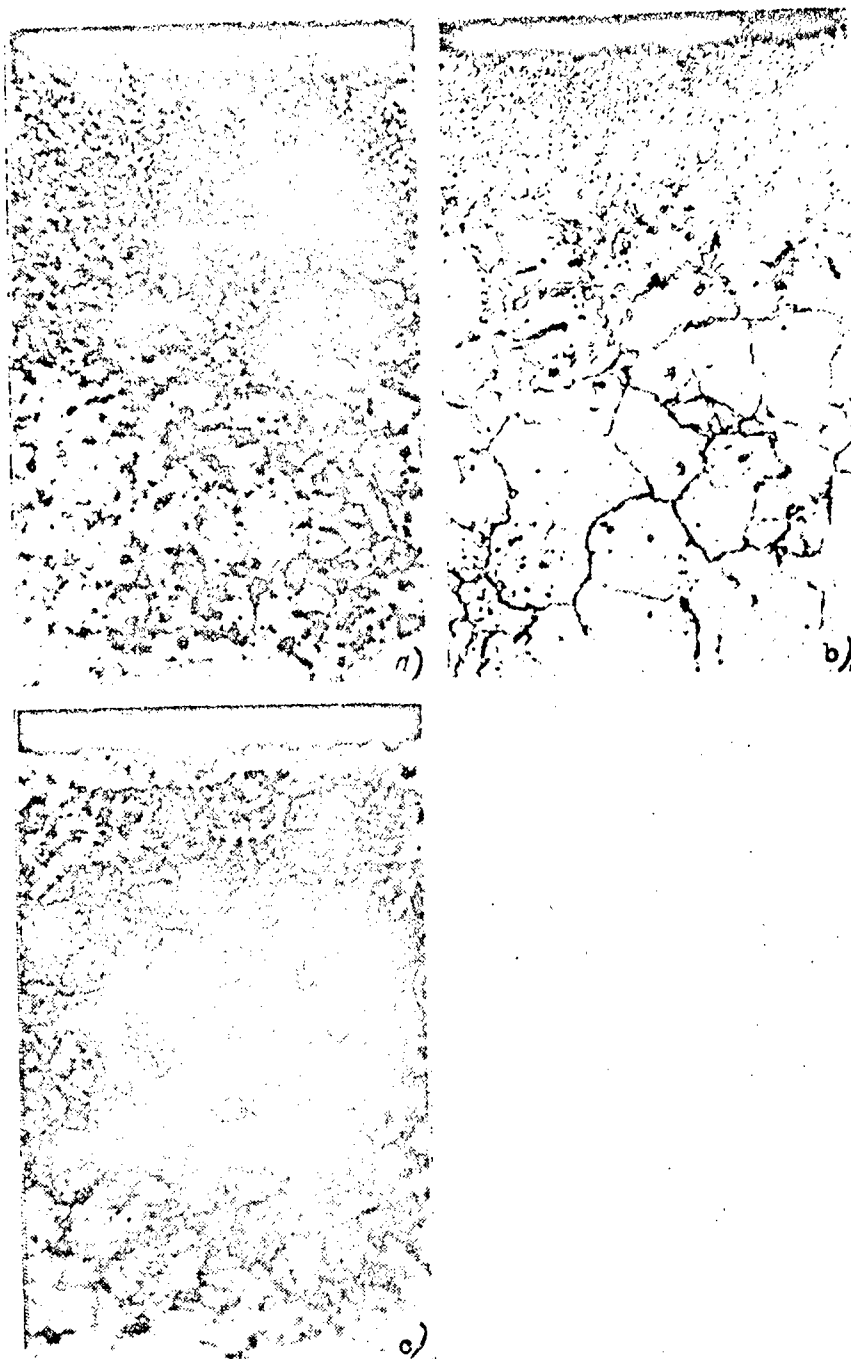


Fig 18. Microstructure of borated steel layer: a - Kh23N18 (boration temperature 950°C); b - Kh23N18 (boration temperature 1,100°C); c - Kh25N25T (boration temperature 950°C); X500

In the saturation of highly complex alloyed steel containing a high content of nickel, chromium, and other components, apparently the formation of the diffusion layer takes place in the following way. After the solid solution has reached its saturation limit with boron and the component alloy, borides appear on the surface being treated. The formation of borides which contain a large amount of boride-producing components, is accompanied by a reduction of these components in the solid solution. The borides appear in the form of individual sections located within the solid solution and exist simultaneously with it. With the passage of time borides are formed not only on the surface but within the layer, and the austenitic-boride (or ferrite-boride) zone extends to a certain depth. Along with an increase in the biphased zone ( $\gamma$  solid solution plus borides) the quantity also increases and there is an increase in the boride formations on the surface and in the layer depth.

The more boride-producing components which the steel contains, the greater is their affinity to boron and the less the boride requires boron for its formation. In addition the remaining conditions being the same, the borides are also formed more readily. As a result, a solid layer of borides is formed on the surface, under which is located a well developed austenitic-boride (ferrite-boride) zone.

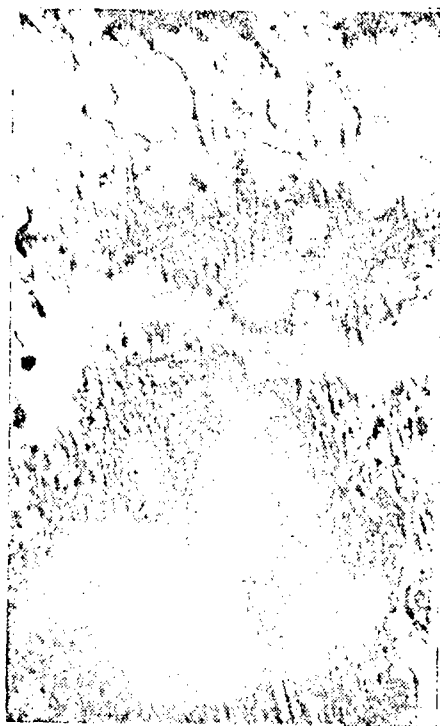


Fig 19. Microstructure of a borated layer of steel containing 0.41%C and 12.82%Ni. X500

Figure 18 shows the microstructures of a borated layer in Kh23N18 and Kh25N25T steel, which illustrates quite well the described mechanism for the formation of the diffusion layer.

Brief saturation with boron at a high temperature leads to the formation of a well developed austenitic-boride zone (Figure 19). In the given case a solid boride layer is not formed due to the intensive discharge of boron atoms (caused by the diffusion processes in austenite) from the surface to deeper layers. With a decrease in the boration temperature and an increase in the length of the process, a solid layer of borides is formed on the surface, under which an austenitic-boride zone (see Figure 18) is formed. In this zone the borides are initially formed along the boundaries and the joints of the austenite grain, then in the grains and along the boundaries of large blocks of mosaic, where metastability of the supersaturated solid solution is apparently attained. This formation of the boride phases provides a basis for assuming that the diffusion of boron takes place primarily along the grain boundaries.

Diffusion along the grain boundaries is usually observed in most cases in which the solubility of the diffusing component in the basic metal is small. Boron is no exception in this case. The increased diffusion mobility of boron along the grain boundaries can be explained by its solubility and by another energy state which are greater than within the grain. Atoms along the boundaries have greater mobility than they do within the grain, due to the high concentration of vacancies. The activation energy of diffusion along the grain boundaries, as has been shown in several studies, is considerably less than for diffusion within the grain.

Along with saturation by boron of the steel surface, carbon is removed from the austenite by means of its diffusion toward the core. This can readily be seen in Figure 19, where the microstructure of a borated layer obtained in steel, containing 0.41%C and 12.82%Ni, is shown.

Thus in the transitional austenite-boride zone at the diffusion temperature there are at least two solid solutions with differing carbon concentrations along with the boride phase.

An X-ray structural study of the phase composition of a borated layer in steel containing a large amount of chromium (13%Cr), steel containing nickel (25%Ni) and steel

containing chromium and nickel (18%Cr and 8%Ni) shows that it consists of iron borides, in which part of the iron atoms are replaced by component alloys (Ref 6).

When steel containing a large amount of chromium is borated, the borides  $(\text{FeCr})_2\text{B}$  and  $(\text{Fe, Cr})\text{B}$ , the nickel borides  $(\text{Fe, Ni})_2\text{B}$  and  $(\text{Fe, Ni})\text{B}$ , and the chromium-nickel borides  $(\text{Fe, Ni, Cr})_2\text{B}$  and  $(\text{Fe, Ni, Cr})\text{B}$  are formed. It is possible that boron is replaced by carbon in the borides.

Similarly with the carbide phase, when steel containing a large amount of boride-producing components - for example, nickel - is saturated with boron, the formation of borides of the type  $\text{Ni}_3\text{B}$  and  $\text{Ni}_2\text{B}$  is possible.

#### THE BORATION OF NICKEL AND ITS ALLOYS

[We found no data in the literature regarding strengthening nickel by the boration method, if we exclude the works of Oknov and Moroz.] (Ref 11).

As can be seen from Table 4 and Figure 20, with nickel boron forms a series of borides.

The borides  $\text{Ni}_3\text{B}$ ,  $\text{Ni}_3\text{B}_2$ , and  $\text{NiB}$ , which are poor in boron, are of great value in studying the structure of a borated layer.]

The boride  $\text{Ni}_3\text{B}$  has a rhombic lattice with the periods  $A = 4.352$ ;  $B = 5.223$ , and  $C = 6.615 \text{ \AA}$  (ref 19). According to R. Stig (Ref 20) the lattice periods of  $\text{Ni}_3\text{B}$  are:  $A = 4.389$ ,  $B = 5.211$ , and  $C = 6.619 \text{ \AA}$ . The boride  $\text{Ni}_2\text{B}$  has a tetragonal lattice of the type  $\text{CuAl}_2$  with the periods:  $A = 4.980$ ;  $C = 7.396$ , and  $C/A = 0.851$  (Ref 21). The nickel boride  $\text{NiB}$ , according to data given by Blum (Ref 22), has an orthorhombic lattice with the periods:  $A = 2.952$ ;  $B = 7.396$ , and  $C = 2.966 \text{ \AA}$ . There are no data in the literature regarding solubility of boron in nickel.

[The formation mechanism of the borated layer in nickel and in iron is the same. The boron initially dissolves in the nickel, and when the limits of solubility are reached on the surface produces a solid boride layer  $\text{Ni}_3\text{B}$ , containing 25-30%Ni. After a period of time a phase recrystallization is possible on the surface with the formation of a boride  $\text{Ni}_2\text{B}$  which is richer in boron.]



The growth of boride phases in the diffusion layer also points to the existence of solid solutions on a boride base and to the solubility of boron in nickel, which is not noted in the composition diagram (see Figure 20). A study which we carried out showed that gas boration in the mixture of diborane with hydrogen  $B_2H_6$  plus  $H_2$ , in the ratio 1:25, is an effective method of strengthening nickel and alloys based upon it. Figure 21 shows a typical microstructure of a borated layer in pure nickel after saturation from the gas phase ( $B_2H_6$  plus  $H_2$ ) at a temperature of 950°C for 6 hours. Thus a well developed solid layer of borides is formed on the surface. This layer is at a depth of 70-80mk, has great hardness, and changes little with depth. A characteristic of such a diffusion layer is the penetration of boride phases along the grain boundaries to a considerable depth. After boration according to the indicated regime borides along the grain boundaries were detected at a depth of more than 1mm. With an increase in the process temperature the depth of the borated layer increases exponentially. The alloys of nickel were also treated to boration. The results are given in Table 6.

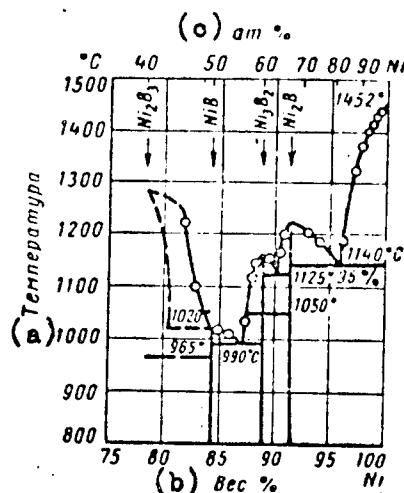


Fig 20. Composition diagram Ni-B.  
a) temperature; b) weight %; c) technical atmosphere %.

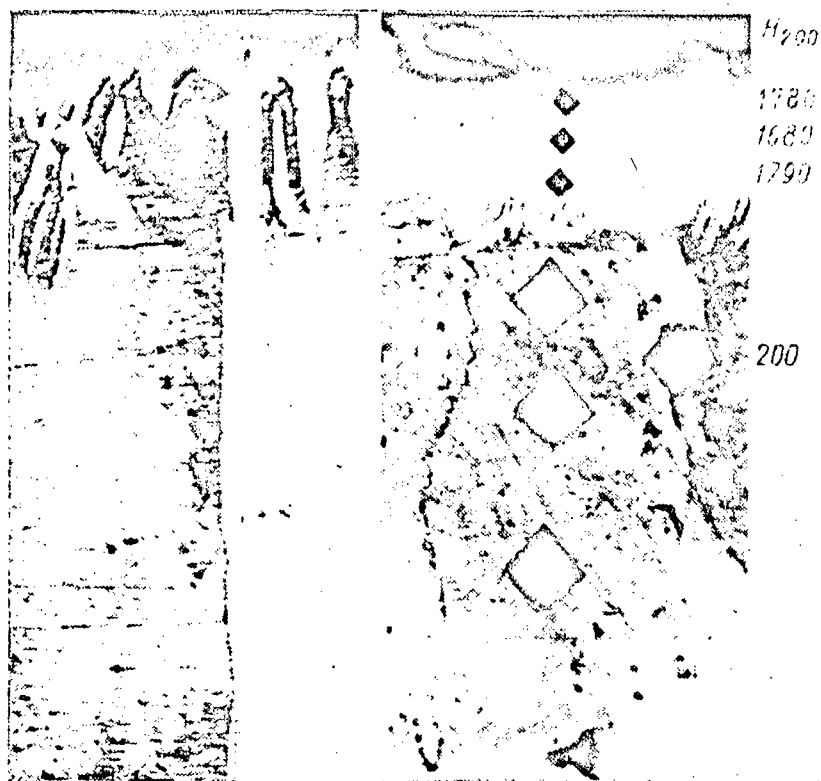


Fig 21. Microstructure of a borated layer in pure nickel. X500

Table 6

(a) Сплав	(b) Режим борирования		(c) Глубина слоя в мк		(h) Микротвер- дость $H_{200}$ на поверх- ности
	(d) Температура в °C	Продолжи- тельность (e) в ч	(f) боридов	(g) общая	
X20N80(i)	900	4	20—25	70—100	1780
X27N70(j)	950	6*	50—60	100—130	1890
X20N70T(k)	950	6*	50	150—180	2010
X16N57(l)	950	6	20	130—150	1830

a) alloy; b) boration regime; c) layer depth in mk; d) temperature in degrees C; e) duration in hours; f) borides; g) total; h) microhardness  $H_{200}$  on the surface\* ; i) Kh20N80; j) Kh27N70; k) Kh20N70T; l) Kh16N57.

\* After boration, diffusion soaking was carried out without the addition of an active mixture ( $B_2H_6$  plus  $H_2$ ) for four hours.

As can be seen from the data which are given, the boration of nickel alloys ensures great surface hardness.

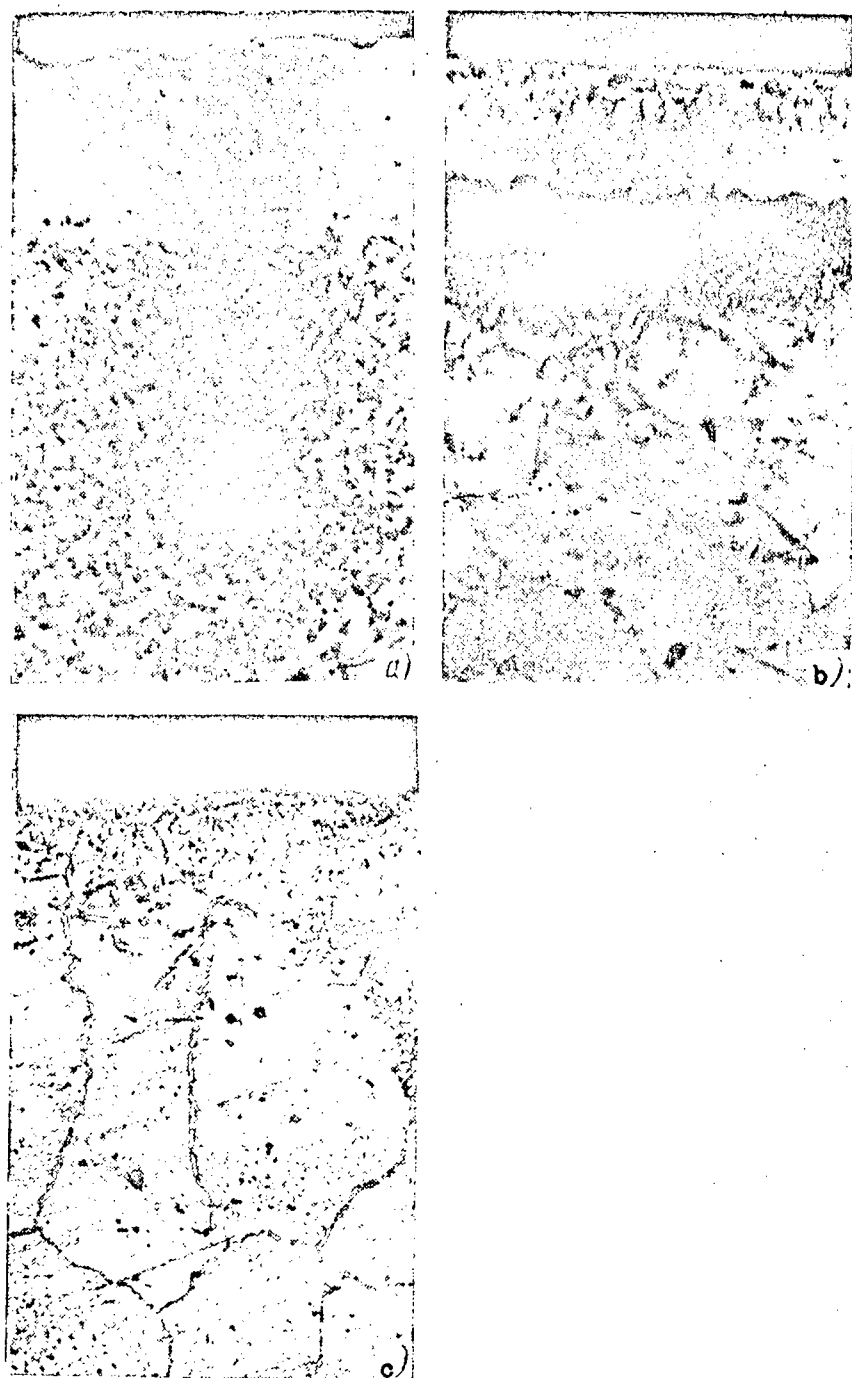


Fig 22. Microstructure of the borated layer obtained for nickel alloys Kh20N70T (a) and Kh27N70 (b) at a temperature of 950°C for 6 hours and for the nickel alloy Kh20N70T (c) at a temperature of 1,100°C for 2 hours. X500.

Figure 22 shows the structure of an alloy on a nickel base, in which the solid layer of borides of the type  $(Ni, Cr)B$  and  $(Ni, Cr)_3B$  can be seen, under which a well developed zone is located: solid solution - borides.

The formation kinetics of a diffusion layer in nickel alloy does not differ in principle from that described for complex alloys on an iron base a layer is first formed on the surface which is composed of a solid solution and borides. If the saturation process is increased, at a given temperature the formation of new boride deposits takes place, which leads to the formation of a solid boride layer on the surface, under which is located a well developed zone made up of a solid solution and boride phases. The higher the temperature, the less the development, other conditions being equal, and layers of solid borides are formed. The zone then greatly increases: solid solution-borides (see Figure 22).

Figure 23 shows the nature of the hardness change depending on the depth of the borated layer in Kh20N70T steel. Within the limits of the solid boride layer, the hardness barely changes; in the transition to a layer composed of a solid solution in borides, the hardness greatly decreases. Fragility of the borated layer is small. The study which was carried out showed that it was completely possible to strengthen the surface of nickel alloys by means of gas boration.

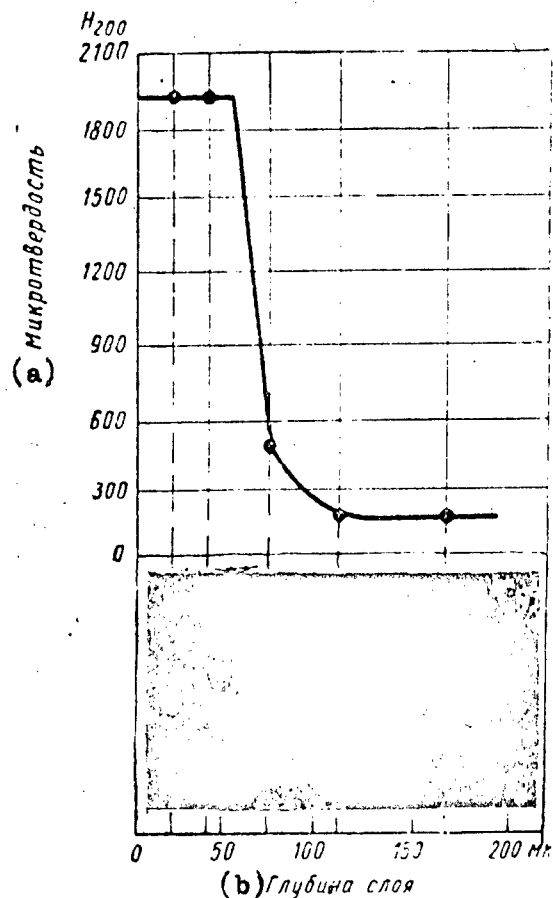


Fig 23. Hardness distribution according to the borated layer of steel Kh20N70T. X200  
a) microhardness; b) layer depth.

### CONCLUSIONS

1. In this study it has been shown that the formation kinetics of the borated layer obeys the general laws of reactive diffusion.

2. It has been established that the diffusion of boron takes place more readily in a body-centered lattice of  $\alpha$ -iron than in a boundary-centered lattice of  $\gamma$ -iron.

Frontal diffusion was observed in the lattice of  $\alpha$ -iron, which corresponds to the development of a borated layer.

3. The phase composition and the formation kinetics of a borated layer in highly complex alloyed steel of the type Kh18N9T, Kh23N18 and Kh25T was studied. It was shown that after saturation of the solid solution a multiphased layer is formed in the diffusion layer; this layer is composed of a solid solution of boron in iron and iron borides of the type  $(\text{Fe}, \text{Cr}, \text{Ni})_2\text{B}$ , and also of lower chromium and nickel borides ( $\text{Cr}_2\text{B}$ ,  $\text{Cr}_4\text{B}$ ,  $\text{Ni}_2\text{B}$ ,  $\text{Ni}_3\text{B}$ , and others). After a period of time a solid boride layer made up of high borides ( $\text{CrB}$ ,  $\text{Cr}_2\text{B}_5$ ,  $\text{NiB}$ ,  $\text{Ni}_3\text{B}_5$ ) and of iron boride of the type  $(\text{Fe}, \text{Cr}, \text{Ni})\text{B}$  is formed on the surface. Under the layer of solid borides a multiphased layer is located (solid solution plus borides) beyond which there is a zone of a solid boron solution in iron.

4. The effect of alloy components (chromium, nickel manganese, niobium, titanium) on the development of the diffusion layer was studied:

a. In steel containing an average amount of carbon (0.3-0.5%C) small additions of chromium sharply decreased layer depth. An increase in the chromium content from 3-8% causes no noticeable change in the over-all depth of the layer or of the layer of solid borides. With a high chromium content (12-15%) a decrease in the depth of the borated layer is again observed;

b. 4-6% nickel decreases the layer depth in steel containing an average amount of carbon, but a higher content of nickel has practically no effect;

c. If steel containing a large amount of chromium, 3Kh15 and 3Kh15V2, is alloyed with nickel, there is an increase in the general layer depth and in the layer depth of solid borides;

d. If 8% manganese is introduced into chromous steel 3Kh15V2 the depth and character of the layer barely changes.

e. Of all the component alloys which were studied niobium and titanium decreased most sharply the depth of the borated layer in Kh18N8 steel.

5. It was found that it is possible to carry out

gas boration of nickel and its alloys. The formation of a diffusion layer in nickel and its alloys takes place in a manner which is similar to the formation in the alloys with an iron base. A change in the phase composition of the diffusion layer from the surface to the depth is characterized in the following way:  $\text{NiB}$  and  $\text{Ni}_3\text{B}_2 \rightarrow \text{Ni}_2\text{B} \rightarrow \text{Ni}_3\text{B}$ .

In nickel alloys of the type Kh20N70, the highest layers ( $\text{NiB}$ ,  $\text{Ni}_3\text{B}_2$ ,  $\text{Cr}_5\text{B}_3$ ,  $\text{Cr}_2\text{B}_5$ ,  $\text{CrB}$ ) were located in the surface layer and the lowest borides ( $\text{Ni}_3\text{B}$ ,  $\text{Ni}_2\text{B}$ ,  $\text{Cr}_2\text{B}$ ,  $\text{Cr}_4\text{B}$ ) were located in the layer located far from the surface, in addition to the nickel borides ( $\text{Ni}$ ,  $\text{Cr}$ )B and ( $\text{Ni}$ ,  $\text{Cr}$ ) $_2\text{B}$ .

#### REFERENCES

1. Khansen, M., Struktura binarnykh Splavov (Structure of Binary Alloys), Vol I, State Publishing House of Literature on Metallurgy, 1941.
2. Mokin, N.P., Izvestiya Sibirskogo instituta metallov (News of the Siberian Institute of Metals), 4th edition, 1934, No 1.
3. Morozova, Ye.M. and Florensova, F.Ye., Sb. statey Laboratorii Metallovedeniya ENIMS (Collection of Articles of the Laboratory of Metal Sciences of the Experimental Scientific-research Institute of Metal-cutting Machine Tools), State Scientific-technical Publishing House of Machine-building Literature [Mashgiz], 1944.
4. Blanter, M.Ye. and Besedin, N.P., Metallovedeniye i Termicheskaya Obrabotka Metallov (Metal Science and Heat Treatment of Metals), 1955, No 6.
5. Lakhtin, Yu.M. and Pchelkina, M.A., Metallovedeniye i termicheskaya obrabotka metallov, Mashgiz, 1960.
6. Zhdanov, G.S., Zhuravlev, N.N. and Zevin, L.S., Doklady AN SSSR (Reports of the Academy of Sciences USSR), Vol 92, 1953, No 4.
7. Samsonov, G.V., Zhurnal Fizicheskoy Khimii (Journal of Physical Chemistry), Vol 32, 1958, No 10.
8. Samsonov, G.V., Zhuravlev, N.N. and Amnuel', I.G., Fiziki Metallov i Metallovedeniye (Physics of Metals and Metal Science), 1956, No 3.
9. Samsonov, G.V., Doklady AN SSSR, Vol 93, 1953, No 5.
10. Samsonov, G.V. and Latysheva, V.P., Doklady AN SSSR, Vol 109, 1956, No 3.



11. Onkov, M.G. and Moroz, L.S., Zh T F (Journal of Technical Physics), Vol XI, Nos 7, 8, 1941.
12. F. Wever, A. Muller, Zeitschr, anorg, Cheme, 192, 317, 1930.
13. T. W. Pretiad, R. Speiser, Journal Metals, 5 No. 3, 1953.
14. M. E. Nicholson, Journ. Metals 4, No. 2, 148, 1952, 6, No. 2, 185, 1954.
15. R.p. E. Busby, M. E. Warga, C. Well, Journ. Metals, 5, No. 14, 1463, 1953.
16. P. E. Busby, C. Wells, Journ. Metals, 6, No. 9, 972, 1954.
17. C. C. McBride, T. W. Pretnak, R. Speiser, Trans., Amer. Soc. Metals, 46, 999, 1954.
18. G. M. Leak, Metal Tseatm. Drop. Forgg, 23, 1956.
19. R. Fruchart, Andri M., Cr. Acad. Sci 245, No. 2, 171-72, 1957
20. R. Stig, Nature, 181 No. 4604, 259-260, 1958.
21. N. J. Wallbaum, Zeitsch. Metall kunde, 35, 218, 1943.
22. P. Blum, Journ. Phys Radium, 13 No. 7/9, 430, 1952.

10,322  
CSO: 1879-S/PE